# Title: Pectin methyltransferase QUASIMODO2 functions in the formation of seed coat mucilage in Arabidopsis

**Authors:** Juan Du[1,#], Mei Ruan[1,#], Xiaokun Li[1], Qiuyan Lan[1], Qing Zhang[1], Shuang Hao[1], Xin Gou[1], Charles T. Anderson[2] and Chaowen Xiao[1]

**Author Affiliations:**
[1]Key Laboratory of Bio-Resource and Eco-Environment of Ministry of Education, College of Life Sciences, Sichuan University, Chengdu 610064, China
[2]Department of Biology, The Pennsylvania State University, University Park, PA 16802, USA

**Author for correspondence:**
Chaowen Xiao, PhD
Key Laboratory of Bio-Resource and Eco-Environment of Ministry of Education, College of Life Sciences, Sichuan University, Chengdu 610064, China
Tel: +(86) 28-85465791; Email: cwxiao@scu.edu.cn

**Running title:** Pectic homogalacturonan functions in seed mucilage formation

**Keywords:** pectin methyltransferase, homogalacturonan, cell wall, cellulose, seed coat mucilage, *Arabidopsis thaliana*

**Title: Pectin methyltransferase QUASIMODO2 functions in the formation of seed coat mucilage in Arabidopsis**

**Authors:** Juan Du[1,#], Mei Ruan[1,#], Xiaokun Li[1], Qiuyan Lan[1], Qing Zhang[1], Shuang Hao[1], Xin Gou[1], Charles T. Anderson[2] and Chaowen Xiao[1]

**Author Affiliations:**
[1]Key Laboratory of Bio-Resource and Eco-Environment of Ministry of Education, College of Life Sciences, Sichuan University, Chengdu 610064, China
[2]Department of Biology, The Pennsylvania State University, University Park, PA 16802, USA

**Author for correspondence:**
Chaowen Xiao, PhD
Key Laboratory of Bio-Resource and Eco-Environment of Ministry of Education, College of Life Sciences, Sichuan University, Chengdu 610064, China
Tel: +(86) 28-85465791; Email: cwxiao@scu.edu.cn

**Running title:** Pectic homogalacturonan functions in seed mucilage formation

**Keywords:** pectin methyltransferase, homogalacturonan, cell wall, cellulose, seed coat mucilage, *Arabidopsis thaliana*

## Abstract

Pectin, cellulose, and hemicelluloses are major components of primary cell walls in plants. In addition to cell adhesion and expansion, pectin plays a central role in seed mucilage. Seed mucilage contains abundant pectic rhamnogalacturonan-I (RG-I) and lower amounts of homogalacturonan (HG), cellulose, and hemicelluloses. Previously, accumulated evidence has addressed the role of pectin RG-I in mucilage production and adherence. However, less is known about the function of pectin HG in seed coat mucilage formation. In this study, we analyzed a novel mutant, designated *things fall apart2* (*tfa2*), which contains a mutation in HG methyltransferase QUASIMODO2 (QUA2). Etiolated *tfa2* seedlings display short hypocotyls and adhesion defects similar to *qua2* and (*tumorous shoot development2*) *tsd2* alleles, and show seed mucilage defects. The diminished uronic acid content and methylesterification degree of HG in mutant seed mucilage indicate the role of HG in the formation of seed mucilage. Cellulosic rays in mutant mucilage are collapsed. The epidermal cells of seed coat in *tfa2* and *tsd2* display deformed columellae and reduced radial wall thickness. Under polyethylene glycol treatment, seeds from these three mutant alleles exhibit reduced germination rates. Together, these data emphasize the requirement of pectic HG biosynthesis for the synthesis of seed mucilage, and the functions of different pectin domains together with cellulose in regulating its formation, expansion, and release.


## Introduction

The cell wall surrounding plant cells not only provides structural support for intracellular constituents, but also regulates plant growth and development. It functions in cell wall integrity maintenance, cell signaling, and response to internal and environmental cues (Caffall and Mohnen, 2009; Vaahtera et al., 2019; Anderson and Kieber, 2020). Pectin, together with cellulose and

xyloglucan, makes up the bulk of primary cell walls in dicotyledonous plants (Zablackis et al., 1995). Pectin is one of the most abundant and complex constituents of the primary cell wall, and is mainly composed of three types of polysaccharides: homogalacturonan (HG), rhamnogalacturonan I (RG-I), and rhamnogalacturonan II (RG-II). HG can be covalently bound to RG-I or RG-II to form pectin macromolecules (Atmodjo et al., 2013). Of the pectin domains, HG, which consists of linear chains of α-1,4-linked galacturonic acid (GalA) residues, is the most abundant. It can be acetylated at the O2 and O3 positions and methylesterified at the C6 carboxyl group (Caffall and Mohnen, 2009). RG-I has a disaccharide repeats backbone composed of α-D-GalA-α-L-Rha with different side chains. The GalA residues in RG-I backbone are also acetylated at O2 or O3, and the Rha residues may be substituted at O4 with oligosaccharides or polysaccharides (Atmodjo et al., 2013). RG-II has an HG backbone substituted with four well-defined side chains. RG-II molecules are known to form RG-II-B dimers via a boron diester bond (Caffall and Mohnen, 2009; Atmodjo et al., 2013). Pectin is biosynthesized in the Golgi apparatus, and highly methylesterified HG is secreted into the apoplast (Staehelin and Moore, 1995) and de-methylesterified by pectin methylesterases (PMEs). PME activity is modulated by pectin methylesterase inhibitors (PMEIs) (Willats et al., 2001). The degree of methylesterification and the distribution patterns of methylesters in HG chains determine binding interactions between pectin and calcium ions ($Ca^{2+}$) that lead to pectin crosslinking, and the ability of pectin-degrading enzymes to bind to HG molecules. Contiguous de-methylesterified GalA may cross link with $Ca^{2+}$ to form “egg box” structures, which are predicted to strengthen wall mechanics and increase cell–cell adhesion (Peaucelle et al., 2012; Hocq et al., 2017). Sporadically de-methylesterified HG can be degraded by polygalacturonases (PGs) and pectate lyases (PLs) to allow for wall expansion (Pelloux et al., 2007; Wolf et al., 2009; Xiao et al., 2014; Rui et al., 2017; Wu et al., 2020).

Pectic HG synthesis requires the participation of different glycosyltransferases, methyltransferases, and acetyltransferases (Mohnen, 2008; Atmodjo et al., 2011). GALACTURONOSYLTRANSFERASE1 (GAUT1) has HG:GalA transferase activity and forms a complex with GAUT7 to accomplish glycan chain elongation (Amos et al., 2018). GAUT8 is also necessary for HG synthesis: mutations in *GAUT8* cause GalA content reduction in the cell wall and cell adhesion defects (Bouton et al., 2002). GAUT11 functions in the formation of seed coat mucilage (Voiniciuc et al., 2018), and GAUT12 not only regulates pectin synthesis, but also affects the deposition of lignin in secondary cell walls, with mutations in *GAUT12* resulting in plant dwarfism (Persson et al., 2007; Hao et al., 2014). In addition to galacturonosyltransferases, several putative pectin methyltransferases such as QUASIMODO2 (QUA2), QUA3, CGR2 (COTTON GOLGI RELATED 2), and CGR3 have been identified to be involved in HG synthesis (Krupkova et al., 2007; Mouille et al., 2007; Miao et al., 2011; Kim et al., 2015). Recently, heterologously expressed PMR5 (POWDERY MILDEW RESISTANT5) was shown to transfer acetyl groups to oligogalacturonides *in vitro* (Chiniquy et al., 2019).

Seed coat mucilage, a specialized type of cell wall, is an excellent system for the investigation of cell wall structure and function (Griffiths and North, 2017). In angiosperms like *Arabidopsis thaliana*, transparent, soluble, and pectinaceous polysaccharides are synthesized and secreted from the seed coat epidermis when mature dry seeds are hydrated in water (Arsovski et al., 2010; Haughn and Western, 2012). The seed coat epidermis stems from the outer ovule integument after fertilization and increases in size by vacuolar expansion. During mucilage deposition, a mucilage pocket is present in the space between the primary cell wall and the developing columella. Following its growth, the columella is delimited by a secondary cell wall and is shaped like a volcano (Western et al., 2000). Once extruded, seed coat mucilage

contains two different layers of structures surrounding the mature seeds: the outer mucilage is diffuse and can be easily extracted by gentle shaking, whereas the inner mucilage adheres tightly to seeds and can be removed only by vigorous shaking. Some evidence has implied that seed coat mucilage facilitates successful seed germination under extreme conditions, which might be beneficial for seed survival, dispersal, hydration, and attachment to soil (Haughn and Western, 2012; Francoz et al., 2015; Ezquer et al., 2016).

Analysis of seed coat mucilage has revealed that it contains many components of primary cell walls, but in unique proportions, including abundant pectic RG-I and lesser amounts of HG with varying degree of methylesterification; cellulose; and hemicelluloses (Windsor et al., 2000; Macquet et al., 2007). Several key enzymes required for RG-I synthesis have been identified to function in seed mucilage production through genetic analysis. MUCILAGE-MODIFIED4/RHAMNOSE BIOSYNTHESIS2 (MUM4/RHM2), a UDP-L-rhamnose synthase, participates in mucilage RG-I synthesis (Oka et al., 2007). It is modulated by upstream regulator APETALA2 (AP2), TRANSPARENT TESTA GLABRA1 (TTG1), and GLABRA2 (GL2) to accomplish seed coat development and mucilage production (Usadel et al., 2004; Western et al., 2004). Mutations in MUCILAGE-RELATED 70 (MUCI70), RUBY PARTICLES IN MUCILAGE (RUBY), β-D-XYLOSIDASE/α-L-ARABINOFURANOSIDASE1 (BXL1), and MUCILAGE-MODIFIED2 (MUM2), which influence the structures of galactan and arabinan side chains on RG-I, result in defective mucilage release (Dean et al., 2007; Arsovski et al., 2009; Voiniciuc et al., 2018; Sola et al., 2019). These findings indicate that pectic RG-I side chains are crucial for normal mucilage release. Aside from RG-I, HG may also function in seed mucilage formation. GAUT11 is required for the synthesis of an HG region attached to RG-I, and *gaut11* mutants show significant reductions in galacturonic acid and rhamnose content in seed mucilage (Voiniciuc et al., 2018). Furthermore,

pectin methylesterification status is associated with seed mucilage formation and release. It appears that a lower degree of methylesterification on HG limits mucilage release to some degree (Rautengarten et al., 2008; Saez-Aguayo et al., 2013; Voiniciuc et al., 2013). Besides containing large amounts of pectic polysaccharides, mucilage also contains some cellulose. CELLULOSE SYNTHASE5 is required for cellulose production and mucilage adhesion in seed coat epidermal cells (Mendu et al., 2011; Griffiths et al., 2015). Cellulose is also the primary constituent of the columella, which arises from seed coat epidermal cells. Normal cellulose deposition in the walls of Arabidopsis seeds is essential for the establishment of subsequent mucilage architecture (Yang et al., 2019). Mucilage attachment to the seed coat is likely dependent on interactions between wall components such as pectin and cellulose that vary spatiotemporally to allow for dynamic behaviors during seed maturation, dispersal, and germination (Western et al., 2000; Stork et al., 2010; Voiniciuc et al., 2015a).

QUASIMODO2 (QUA2), a pectin methyltransferase, has been demonstrated to be involved in HG synthesis. Two mutant alleles of *QUA2*, *quasimodo2* (*qua2*) and *tumorous shoot development2* (*tsd2*), show reduced pectin HG content, severe cell–cell adhesion defects, and growth inhibition (Krupkova et al., 2007; Mouille et al., 2007; Du et al., 2020). However, little is known about the function of QUA2 in pectin synthesis and modification during seed mucilage formation. In this study, a novel allelic mutant of *qua2* and *tsd2*, referred to as *tfa2* (*things fall apart2*), was characterized. Besides showing shorter hypocotyls and cell adhesion defects in hypocotyl epidermal cells, we observed that *QUA2* allele mutants have reduced pectin content and methylesterification degree, and display structural defects in seed coat mucilage. *tfa2* with *tsd2* and *qua2* mutant seeds exhibit lower levels of crystalline cellulose compared with wild-type. The surface morphology of seed coat in mutants is altered, showing deformed volcano-shaped columellae,

along with decreased germination rates under low water availability. These results indicate that QUA2 is involved in the formation of seed mucilage, and provide new evidence to support the function of homogalacturonan in the deposition of seed mucilage.

## Materials and methods

### *Plant materials and growth conditions*

*Arabidopsis thaliana* ecotype Colombia (Col-0), *tfa2*, *tsd2*, and *qua2* mutant seeds were used in this study. Three *QUA2* allele mutant seeds were kindly provided by Tanya Falbel and Sara Patterson. Seeds were surface sterilized in 30% bleach containing 0.1% SDS, followed by washing four times with sterile water. After sowing on Murashige and Skoog (MS) plates containing 2.2 g/L MS (Phytotech lab, Cat#M519), 0.6 g/L MES (Life-biotech, Cat#A610341-0100), 1% or 0% (w/v) sucrose, and 0.8% (w/v) agar, pH 5.6, seeds were vernalized at 4°C in the dark for 4 days. Seedlings were grown in a chamber at 22°C with a 16-h-light/8-h-dark photoperiod for 8 days. Then seedlings were transferred from MS medium plates into sterilized soil, and grown in a greenhouse under the same conditions. The seeds of different genotypes are from the same batch and harvested after full maturation and complete drying.

### *Construction of complementary plants*

For generation of complementary plants, fragments of 2.0 kb upstream of QUA2 translation initiation site from Col genomic DNA and the full length of *QUA2* coding sequence from Col leaf cDNA were amplified by high-fidelity DNA polymerase with gene-specific primers (Table S1). Two PCR fragments were integrated into the binary vector pH7FGW2 to generate the *QUA2pro::QUA2* construct, which was transformed into *Agrobacterium tumefaciens* strain GV3101 and infected *tfa2* mutant plants using the floral dip

method (Clough and Bent, 1998). Positive transformants were selected on MS plates containing 25 μg/mL hygromycin.

## *Hypocotyl length measurements and epidermal cell morphology*

For observations of hypocotyl length, MS plates containing 6-day-old dark-grown seedlings were scanned by a HP Scanjet G4050 scanner at 600 dpi, and hypocotyl length was measured in ImageJ. Cell adhesion defects were observed and analyzed by imaging hypocotyl epidermal cells of etiolated seedlings using a Cell Observer SD spinning-disk confocal microscope with a 100× 1.40 NA oil-immersion objective (Zeiss).

## *Total RNA isolation and gene expression analysis*

Arabidopsis wild-type flowers at the day of pollination were carefully labeled as previously described (Western et al., 2000). Rosette leaves from 6-week-old adult plants and siliques at the day indicated were collected and used for the extraction of total RNA using a Plant RNA Kit (Omega). RNA samples were treated with RNase-free DNase I (NEB) on a column to remove genomic DNA. RNA concentration was measured by spectrophotometer (NanoDrop™ One$^{C}$), and first-strand cDNA was synthesized from 500 ng DNase I-treated total RNA using PrimeScript$^{TM}$ RT reagent Kit supplemented with a primer mix of random hexamer and oligo (dT) (Takara, Cat# RR047A). qPCR was performed using SYBR Green FastMix (Takara) with cDNA and gene-specific primers (Table S1) on a Bio-rad CFX96 Touch Real-Time PCR machine. *ACT2* was amplified as an internal control. Gene expression levels were calculated relative to *ACT2* using the ΔΔCT method.

## *Seed size measurements and water absorbance analysis*

About 100 dry seeds of each genotype were imaged with a stereomicroscope (Leica M205FA), and seed area was measured by ImageJ. To explore the water absorption capability of seeds, 100 mg of dry seeds of

each genotype were hydrated in 1.5 mL Eppendorf tubes containing 1 mL water overnight at room temperature to allow seeds to absorb water completely, and the total height of the seeds in the tube after water absorption was measured.

### *Ruthenium red staining and extraction of seed coat mucilage*

Pectin staining of seed coat mucilage was performed according to the method described by Voiniciuc et al. (Voiniciuc et al., 2015a). Staining was carried out in 24-well cell culture plates. Around 30 seeds were placed into a well prefilled with 500 µL water and shaken for 30 min at a speed of 125 rpm (ORBITAL SHAKER KB-900). After removing the water, seeds were stained in a solution of 500 µL 0.01% (w/v) Ruthenium Red (Sigma-Aldrich, Cat#R2751) for 10 min. The dye was removed before washing seeds with water. Then, 500 µL water was added to each well and the seeds were imaged with a stereomicroscope (Leica M205FA). Image processing and quantification of mucilage area were performed in ImageJ according to the method described by Voiniciuc et al. (Voiniciuc et al., 2015a). Total area of seed plus mucilage and seed area were measured by particle function analysis (circularity 0.5–1), respectively. Area of mucilage was calculated by subtracting seed area from total area.

The mucilage extraction was performed as previously described (Xu et al., 2022) with small modifications. Briefly, 100 mg dry seeds were imbibed with 4 mL of distilled water in a 15 mL centrifugal tube and shaken at 200 rpm for 1 h at room temperature. The supernatants were collected by centrifugation at 5000 rpm for 1 min, then the seeds were washed with 1 mL of distilled water. The supernatants were transferred into a 50 mL centrifugal tube and labeled as non-adherent mucilage (NM). The washed seeds were resuspended in 4 mL of distilled water and subjected to ultrasonic treatment (65% amplitude, 6 × 10 s for 1 min) by ultrasound equipment with a 4 mm probe. The supernatants

were collected by centrifugation at 5000 rpm for 1 min, then the seeds were washed with 1 mL of distilled water. The supernatants were collected into a 50 mL centrifuge tube and labeled as adherent mucilage (AM). Then, five times the volume of ethanol was added into NM and AM to precipitate the polysaccharides on ice for 30 min (Mendu et al., 2011). Finally, pellets were collected by centrifugating at 10,000 rpm for 10 min, followed by drying at 45°C and weighing.

## *Determination of degree of pectin methylesterification*

To extract seed mucilage, 5 mg of dry seeds was vigorously vortexed (Scientific Industries Vortex-Genie 2) in 300 µL of 50 mM EDTA for 60 min. After seeds were allowed to settle for 2 min, 250 µL of supernatant was transferred to a new tube and saponified with 0.25 M NaOH for 60 min. The reaction was neutralized with 0.25 M HCl and centrifuged at 10,000*g* for 5 min. An aliquot of 500 µL of neutralized supernatant was transferred into a new 1.5 mL tube, and 500 µL HEPES buffer (pH 7.0) containing 0.5 units of alcohol oxidase (Sigma-Aldrich, Cat#A2404) was added. The solution was then shaken at 250 rpm for 15 min at room temperature. After being briefly centrifuged, 500 µL of assay buffer (20 mM acetyl acetone, 50 mM acetic acid, 2 M ammonium acetate) was added to react at 60°C for 15 min. After cooling down, 1 mL reaction solution was used to read absorbance at 412 nm, and released methanol content was calculated according to a standard curve of methanol (Klavons and Bennett 1986). An aliquot of 200 µL of remaining mucilage solution was used to assay uronic acid content. Absorbance was measured at 525 nm, and uronic acid content was quantified using D-(+)-galacturonic acid monohydrate (Sigma-Aldrich, Cat#48280) as a standard.

## *Immunofluorescence microscopy*

Dry seeds were imbibed in water in a cell culture plate overnight at room

temperature before immunostaining. Imbibed seeds were incubated with primary antibody (Agrisera; JIM5, Cat#AS184194; JIM7, Cat#AS184195) in phosphate buffer containing 3% (w/v) nonfat milk for 1 h at room temperature. After washing three times with PBS buffer, seeds were incubated with DyLight™ 488-labeled goat anti-rat secondary antibody (1:500, SeraCare) in phosphate buffer containing 3% nonfat dry milk for 1 h at room temperature. Negative controls were processed without primary antibody. Fluorescence images were taken using Observer SD spinning-disk confocal microscope with a 488-nm excitation laser and 525/550-nm emission filter (Zeiss).

### *Cellulose content measurements and cellulose staining in seeds*

Cellulose content in seeds was measured according to the method described by Xiao et al. (Xiao et al., 2016) with some modifications. Seeds were ground into a fine powder in liquid nitrogen before washing with 75% ethanol for 45 min at 70°C. The powder was washed with acetone five times, for 2 min each time. The materials were air-dried in a chemical fume hood overnight. An aliquot of 2 mg of air-dried samples was added to a 1 mL solution of acetic acid:water:nitric acid (8:2:1). After vortexing, samples were boiled for 30 min and cooled on ice. The supernatant was discarded by centrifugation for 5 min, and the pellets were washed in 1 mL water. After washing with 1 mL acetone, the pellets were air-dried overnight in a chemical fume hood. An aliquot of 1 mL 67% sulfuric acid was added to resuspend the pellets by vortexing. An aliquot of 50 µL of each sample was added to a tube to which 450 µL of water had already been added. An aliquot of 1 mL 0.2% (w/v) anthrone (Sigma-Aldrich, Cat#319899) in concentrated sulfuric acid was added and vortexed immediately to mix. The samples were heated at 100°C for 5 min, and cooled down to room temperature. Absorbance of samples at $OD_{620}$ was measured using a spectrophotometer (NanoDrop™ One$^{C}$). D-glucose (Sigma-Aldrich, Cat#G8270) was used as a standard to calculate cellulose content.

Cellulose staining was carried out according to a method described by Mendu et al. (Mendu et al., 2011). Around 20 dry seeds were hydrated in 500 µL water in a 24-well plate well for 5 min. The water was removed, and cellulose was stained with 0.01% (w/v) Direct Red 23 (Pontamine Fast Scarlet 4B, Sigma-Aldrich, Cat#212490) in a solution with 50 mM NaCl. After shaking for 60 min at 125 rpm in the dark, seeds were washed three times with 500 µL water and imaged at 561 nm with a confocal microscope (Zeiss). Whole seeds were also stained with Calcofluor White (Sigma-Aldrich, Cat#18909) in a drop of 10% (v/v) KOH for 5 min in dark according to product manual. Seeds were imaged at 405 nm with a confocal microscope (Zeiss).

### *Scanning electron microscopy*

For observation of seed surface morphology, mature seeds of wild-type and mutants were dried at 37°C overnight before being gold-coated with a sputter coater. Seed epidermal cells were scanned with a scanning electron microscope at 1.5 kV (Thermo Scientific Helios G4 UC).

### *Seed germination analysis*

About 50 seeds were placed on moistened paper in a Petri dish with 1 mL water or 10% (w/v) polyethylene glycol PEG-3350 (Sigma-Aldrich). Seeds were stratified at 4°C for 3 days and then grown for 4 days at 22°C under 16 h light/8 h dark conditions. Seed germination was scored every day as testa rupture preceding radicle protrusion.

## Results

### *tfa2, a novel mutant allele of QUA2, displays shorter hypocotyls and cell adhesion defects*

The *qua2* and *tsd2* alleles of *QUA2* are point mutants. Both mutations lead to premature termination of translated peptide (Krupkova et al., 2007; Mouille

et al., 2007). A novel mutant allele isolated via ethyl methanesulfonate (EMS) mutagenesis, called *things fall apart2* (*tfa2*), was identified to contain a mutation in *QUA2* gene by map-based cloning (kindly provided by Tanya Falbel and Sara Patterson). Through PCR amplification and Sanger sequencing of the *QUA2* genomic DNA, a single nucleotide change at 1210 (G to A) was confirmed. This mutation is located in the third exon of coding sequence and generates a stop codon and premature termination (Fig. 1A; Fig. S1; Table S1).

Rapid-growing etiolated seedlings in dark are mainly composed of primary cell walls. Thus, the hypocotyl elongation of etiolated seedlings is considered a good model to study primary cell wall. As previously reported, *qua2* and *tsd2* mutants show shorter hypocotyls and cell adhesion defects in epidermal cells of hypocotyls and cotyledons (Krupkova et al., 2007; Mouille et al., 2007; Du et al., 2020). To determine whether the *tfa2* mutation also affects hypocotyl elongation and cell adhesion, we grew *tfa2* seeds together with *tsd2*, *qua2*, and wild-type seeds on 1/2 MS medium plates in the dark. Hypocotyls of 6-day-old etiolated *tfa2*, *tsd2*, and *qua2* seedlings had average lengths of 1.19 ± 0.25 cm (SD), 0.45 ± 0.14 cm (SD), and 0.59 ± 0.13 cm (SD), respectively, whereas wild-type Colombia (Col) hypocotyls had an average length of 1.78 ± 0.24 cm (Fig. 1B and C). Average hypocotyl length in the three mutant alleles was significantly shorter than Col ($P < 0.001$, *t*-test). The *tsd2* seedlings showed the shortest hypocotyls, whereas *tfa2* hypocotyls were longer than *tsd2* and *qua2* hypocotyls. Similar to *qua2* and *tsd2*, epidermal cells of *tfa2* etiolated hypocotyls also displayed cell–cell adhesion defects (Fig. 1D), although these were relatively milder in *tfa2* seedlings. Among the three mutant alleles, the degree of severity of cell adhesion defects in hypocotyl epidermal cells is correlated with hypocotyl length, suggesting that cell adhesion defects might somehow disrupt hypocotyl elongation. To confirm the observed defects in *tfa2* mutants were caused by loss of function of *QUA2*,

wild-type *QUA2* gene driven by endogenous promoter was expressed in *tfa2* mutant to generate complementary plants (COM). Six-day-old etiolated seedlings of two independent complementary lines had significantly longer hypocotyls than *tfa2* mutant (Fig. S2A and B), and had intact hypocotyl epidermal cells (Fig. S2C), which indicates *QUA2* can rescue shorter hypocotyls and cell adhesion defects of *tfa2* mutants. These data stress the roles of *QUA2* in cell elongation and cell adhesion. Additionally, seedlings of *tfa2*, *tsd2*, and *qua2* mutants had shorter primary roots than Col seedlings (Fig. S3A). The cotyledons of mutant seedlings were prone to be aberrantly hydrated when grown on MS plates (Fig. S3B), likely resulting from cell adhesion defects in the epidermis. When seedlings were transferred into soil to continue growth in a chamber, mutant plants were smaller than wild-type plants (Fig. S3C).

## *tfa2 and tsd2 mutant seeds have altered water absorption capability*

Aside from inhibition of etiolated seedling growth and cell adhesion defects (Fig. 1B and D), we noticed that mutations in *QUA2* influenced the water absorption capability of seeds (Fig. 2). We weighed 100 mg dry seeds of Col, *tfa2*, *tsd2*, and *qua2*, and incubated each batch of seeds with 1 mL water at room temperature overnight to allow the seeds to absorb water completely. Imbibed *tfa2* and *tsd2* seeds displayed smaller total volumes than wild-type seeds (Fig. 2A–C). To determine whether the lower imbibed seed volume in the mutants arises from smaller seed size, we measured the sizes of dry seeds, and found no significant differences between the mutants and wild-type (Fig. 2D). This suggests that the alteration of hydrated seed volume in the mutants is likely due to a diminished ability to absorb water. Considering that alterations in hydrated seed volume are often associated with changes in released seed coat mucilage (Harpaz-Saad et al., 2012; Ben-Tov et al., 2015), we speculated

412 that QUA2 might function in the formation of hydratable mucilage by seed coat
413 epidermal cells.

414 ## *tfa2 and tsd2 mutants show seed coat mucilage defects*

415 To explore the function of QUA2 in seed mucilage formation, we first
416 estimated the expression of *QUA2* in siliques at different developmental
417 stages by real-time quantitative RT-PCR (qPCR). It was found that *QUA2* is
418 expressed at relatively low level in rosette leaves and young siliques at 4 days
419 after pollination (DAP). By contrast, *QUA2* transcripts are dramatically induced
420 at 7, 10, and 13 DAP (Fig. S4A), which is correlated with the time of mucilage
421 formation (Western et al., 2000). Previously published laser-capture
422 microdissection followed by ATH1 GeneChip analysis showed *QUA2* mRNA is
423 expressed throughout seed development and especially enhanced in seed
424 coat at linear cotyledon stage (Fig. S4B) (Winter et al., 2007; Le et al., 2010).
425 This expression pattern in developing seeds supports the idea that QUA2
426 functions in seed development and seed mucilage formation.

427 Thus, we examined whether mucilage deposition, structure, and/or adhesion
428 were affected in *tfa2*, *tsd2*, and *qua2* mutant seeds by ruthenium red staining.
429 Both *tfa2* and *tsd2* seeds showed obviously reduced adherent mucilage when
430 hydrated in water for 30 min, whereas *qua2* seeds released similar amounts of
431 mucilage as wild-type seeds (Fig. 3A and B). Meanwhile, we also directly
432 weighed the released adherent mucilage, which confirmed that *tfa2* and *tsd2*
433 seeds secreted significantly less mucilage than wild-type and *qua2* seeds after
434 soaking in water (Fig. 3C). In parallel, the extruded seed coat mucilage in two
435 complementary lines of *QUA2pro::QUA2/tfa2* was significantly larger than that
436 in *tfa2* mutant seeds (Fig. S5), which indicates wild-type *QUA2* can rescue the
437 seed coat mucilage defects of *tfa2* mutant. However, as the weight of
438 non-adherent mucilage was very low from the seeds of all four genotypes, we
439 failed to obtain accurate weight for them. So we performed the ruthenium red

staining to observe the non-adherent mucilage. As shown in Fig. S6, no obvious difference in non-adherent mucilage was evident between wild-type and mutant seeds upon hydrating dry seeds directly in ruthenium red staining buffer. These data indicate that QUA2 modulates the formation of adherent mucilage.

## *QUA2 is critical for pectin homogalacturonan production and methylesterification in seed coat mucilage*

Mucilage defects are often accompanied by alteration of pectin methylesterification status (Rautengarten et al., 2008; Saez-Aguayo et al., 2013; Voiniciuc et al., 2013). Arabidopsis QUA2 is a pectin methyltransferase, which transfers methyl group to galactosyluronic acid residues in pectin *in vitro* (Du et al., 2020). Loss of function of *OsTSD2*, one of the homologs of Arabidopsis *QUA2* in rice, resulted in a reduced degree of methylesterification in root (Qu et al., 2016). This evidence led us to further investigate whether the degree of methylesterification is altered in seed mucilage of Arabidopsis *QUA2* mutants. As described by previous study, saponification of mucilage-derived alcohol insoluble residue (AIR) was performed and followed by the determination of released methanol through oxidation by alcohol oxidase (Klavons and Bennett, 1986; Louvet et al., 2011). The degree of pectin methylesterification was then calculated as the ratio of released methanol to uronic acid in the AIR. Compared with wild-type, uronic acid content was lower in imbibition-released mucilage for *tfa2* and *tsd2* mutants (Fig. 4A), which is consistent with the result of ruthenium red staining (Fig. 3A). The amount of methanol released from seed coat mucilage-derived AIR was even lower in *tfa2*, *tsd2*, and *qua2* seeds (Fig. 4B), resulting in significantly lower calculated degrees of HG methylesterification in the mutants compared with wild-type controls (Fig. 4C). Immunolabeling experiments were also carried out using JIM5 and JIM7 antibodies, which recognize lower-methylesterified and

higher-methylesterified HG, respectively (Goubet and Mohnen, 1999; Willats et al., 2001). There was noticeably more JIM5 immunofluorescence signal in *tfa2* and *tsd2* seed coat mucilage, but no significant difference in JIM7 immunofluorescence signal in three mutants compared with wild-type controls (Fig. 4D–F). Taken together, these observations indicate that QUA2 is required to maintain proper pectin methylesterification in seed mucilage, and those mutations in *QUA2* increase the proportion of de-methylesterified HG.

## *Mutations in QUA2 hinder the formation of cellulosic rays in seed mucilage*

Previous studies have shown that cellulose is important for both mucilage extrusion and adherence in epidermal cells of seed coats (Griffiths et al., 2014; Griffiths et al., 2015). A recent study found that pectin HG deficiency in etiolated seedlings and adult leaves of *qua2* and *tsd2* mutants inhibits cellulose biosynthesis (Du et al., 2020). To further test the effects of pectin deficiency on cellulose deposition in seed mucilage, we measured crystalline cellulose content in seeds, finding that cellulose content was 44% lower in both *tfa2* and *tsd2* mutant seeds, and 30% lower in *qua2* seeds, than in Col controls (Fig. 5A). Pontamine Fast Scarlet 4B (S4B, also called Direct Red 23) and Calcoflour White are dyes that have been widely used to stain cellulose (Anderson et al., 2010; Xu et al., 2020). Both S4B and Calcoflour White staining revealed that cellulose was collapsed in mucilage capsules of *tfa2* and *tsd2* seeds hydrated in water (Fig. 5B) and produced lower fluorescence intensity (Fig. 5C and D). Meanwhile, the expression of *QUA2* partially rescued the defect of cellulose deposition in the seed mucilage of *tfa2* mutant (Fig. S7A, B). These data indicate that loss of function of *QUA2* restricts cellulose deposition and accumulation in seed mucilage, emphasizing that pectin and cellulose function collectively in generating seed coat mucilage.

## *Surface morphology is altered in tfa2 and tsd2 seed coats*

During seed coat development, production and polar secretion of mucilage results in the formation of a volcano-shaped columella in the center of each epidermal cell (Arsovski et al., 2010). To explore whether the mucilage defects observed in *QUA2* mutants might result from a disruption in this secretory process, seed coat epidermal cells in dry seeds were imaged by scanning electron microscopy (SEM). The images showed that volcano-shaped columellae in both *tfa2* and *tsd2* seeds were severely deformed (Fig. 6A–C), resulting in larger columella areas in three mutants (Fig. 6D), whereas the radial cell walls were thinner than in wild-type controls (Fig. 6E). Surfaces of dry seeds were also observed using bright field mode on a confocal microscope, and we likewise found that columellae on epidermal cells in *tfa2* and *tsd2* mutant seeds were less protrusive than in Col controls (Fig. 6F and G), while the columellae on the seed surface of complementation lines (COM-1 and COM-2) are likely more protrusive than in *tfa2* mutant seeds (Fig. S8). These results underscore the functional requirement for QUA2 in the development and formation of columellae in seed coat epidermal cells, which are essential for normal seed imbibition and germination.

## *QUA2 mutant alleles display reduced seed germination capability under low water availability*

The development of seed epidermal cells and mucilage deposition are closely linked to seed hydration and germination under harsh conditions (Western, 2012). Pectin methylesterification status in cell wall has been shown to influence seed germination (Muller et al., 2012). According to the above analyses, *QUA2* mutants display the defect of mucilage formation, altered degree of methylesterification in released mucilage, and abnormal development in the seed coat epidermis. These findings raised the question of whether seed germination is affected in *QUA2* mutants. As shown in Figure 7, there was no difference in germination rate among tested genotypes when

seeds were grown on normal Murashige and Skoog medium. To find out whether drought stress has an effect on seed germination of mutants, we sowed seeds on the medium supplemented with 10% polyethylene glycol to mimic water-deficient conditions (Ezquer et al., 2016). The results showed that all mutant alleles had lower seed germination rates than Col controls when seeds were exposed to medium supplemented with 10% polyethylene glycol. Notably, *tfa2* seeds displayed almost 50% less germination after 24 h of growth on plates containing 10% polyethylene glycol (Fig. 7). These results imply that QUA2 is required to facilitate seed imbibition and therefore germination, especially under water-limiting conditions.

## Discussion

QUASIMODO2 was first identified as a putative pectin methyltransferase, with functions in mediating cell–cell adhesion and plant development (Krupkova et al., 2007; Mouille et al., 2007). Our recently published results biochemically confirmed that QUA2 possesses pectin methyltransferase activity *in vitro* and is required for normal pectin and cellulose biosynthesis in Arabidopsis (Du et al., 2020). Here, we observed that, apart from its influence on cell adhesion and hypocotyl elongation, QUA2 also functions centrally in seed development and mucilage formation. Previous data have deduced that total seed volume upon hydration in water results from gaps between seeds where gel-like mucilage expands (Harpaz-Saad et al., 2012). Our data show that the water absorption capacity of *tfa2* and *tsd2* mutant seeds is significantly lower than that of wild-type seeds, whereas the size of dry mutant seeds is similar to that of wild-type (Fig. 2), implying a change in seed coat mucilage of *QUA2* mutants (Mizzotti et al., 2014). Indeed, we found that the formation of seed mucilage in mutants, at least *tfa2* and *tsd2* seeds, was inhibited (Fig. 3A and B). These data support a requirement for QUA2 in the production of seed mucilage.

552 Defects in seed coat mucilage are generally associated with changes in the
553 morphology of seed coat epidermal cells (Voiniciuc et al., 2018). The defects in
554 pectin HG content and seed mucilage formation we observed in *QUA2*
555 mutants prompted us to observe the surface morphology of the seed coat
556 epidermis. The SEM images showed that mutant seeds have collapsed and
557 wider volcano-shaped columellae (Fig. 6), around which seed coat mucilage is
558 secreted. The alterations of seed coat properties in mutants further strengthen
559 the link between epidermal cell morphology and mucilage formation in seeds.
560 The data also indicate that QUA2 functions in seed development and the
561 formation of seed coat mucilage by facilitating normal HG biosynthesis.

562 Pectin, relative to other cell wall components, such as cellulose, is the most
563 predominant component of seed coat mucilage (Windsor et al., 2000; Macquet
564 et al., 2007). Among different pectin domains, RG-I is the most abundant in
565 Arabidopsis seed coat mucilage, and has been shown to be essential for the
566 normal formation of seed mucilage, although seed mucilage is also known to
567 contain HG (Macquet et al., 2007; Voiniciuc et al., 2013; Voiniciuc et al.,
568 2015b). However, the precise function of HG in seed coat mucilage remains to
569 be determined. GAUT11 is an HG α-1,4 GalA transferase, and might also
570 function in RG-I chain elongation, despite the RG-I backbone consisting of
571 alternating GalA and rhamnose residues. Mutation of *GAUT11* results in
572 defects in uronic acid content and mucilage extrusion in seeds (Caffall et al.,
573 2009; Voiniciuc et al., 2018), suggesting that HG synthesis influences seed
574 mucilage formation. Besides galacturonosyltransferases, pectin
575 methyltransferases have been shown to function in HG biosynthesis
576 (Krupkova et al., 2007; Mouille et al., 2007; Du et al., 2020). Here, we found
577 that *tfa2* and *tsd2* seeds show smaller mucilage capsules upon water
578 absorption compared with wild-type seeds as revealed by ruthenium red
579 staining and quantification of extracted mucilage (Fig. 3), and significantly less
580 uronic acid is extracted from seed mucilage of *tfa2* and *tsd2* mutants (Fig. 4A).

One interpretation of these results is that the mucilage defect in *QUA2* mutants arises from a reduction in HG content. However, the mucilage extrusion of *qua2* mutant is comparable to wild-type, possibly because the mutation position of *qua2* is located in C-terminus of coding sequence, which keeps relatively intact methyltransferase 29 domain with SAM binding region. Additionally, we cannot completely exclude the possibility that *tfa2* contains other gene interruption in addition to the *QUA2* locus that may partially contribute to seed mucilage defect.

Previous work has demonstrated that the methylesterification level of HG is important for determining mucilage structure and extrusion (Rautengarten et al., 2008; Saez-Aguayo et al., 2013; Voiniciuc et al., 2013; Xu et al., 2020). *tfa2* and *tsd2* seeds show stronger JIM5 immunolabeling signal and a lower degree of methylesterification (Fig. 4), indicating a relatively higher accumulation of low-methylesterified pectin in mucilage of mutant seeds. We also note the significantly altered methylesterification level of remaining HG in seed mucilage of *tfa2*, *tsd2*, and *qua2* alleles (Fig. 4), which was not detected in etiolated seedlings and mature leaves (Krupkova et al., 2007; Mouille et al., 2007; Du et al., 2020). It is possible that QUA2 functions non-redundantly in seed development, whereas other HG methyltransferases such as CGR2 and CGR3 might methylesterify HG in other tissues (Kim et al., 2015). This finding highlights the idea that pectin methylesterification status can be organ-dependent, as found in another study (Xu et al., 2020).

Cellulose has also been demonstrated to play a significant role in maintaining seed mucilage structure, especially in the formation of cellulosic rays and the secondary wall structure called the columella (Sullivan et al., 2011; Griffiths et al., 2014; Ben-Tov et al., 2015; Hu et al., 2016). A previous study showed that cellulose biosynthesis and deposition are defective in hypocotyls of *qua2* and *tsd2* etiolated seedlings (Du et al., 2020). Here, we measured cellulose content in seeds by a biochemical method (Updegraff, 1969). All

three mutants exhibited decreased crystalline cellulose content in their seeds (Fig. 5A). Meanwhile, both hydrated *tfa2* and *tsd2* seeds showed obviously reduced cellulose rays after S4B and Calcofluor White staining (Fig. 5B), which could be caused by reduced cellulose content (Sullivan et al., 2011), or the lack of normal organization of cellulose in the ray (Griffiths et al., 2014). These data indicate that the defective pectin biosynthesis and reduced degree of pectin methylesterification in *QUA2* mutants also have an impact on cellulose deposition in seeds.

The deposition of cellulose, the main component of the volcano-shaped columellae, in the seed coat epidermis is guided by accumulated pectin (Griffiths et al., 2015; Voiniciuc et al., 2015b). The SEM images showed that *QUA2* mutant seeds have thinner radial cell walls, with collapsed and wider columellae. The results in this study support multiple functions for QUA2 in cell wall deposition, ray formation, radial wall thickening, and columella formation during seed coat development. Our previous work has also revealed that mutation of *QUA2* affects microtubule organization in hypocotyl cells (Du et al., 2020). The twisting growth in hypocotyls of microtubule-associated mutants can be restored by inducing cell–cell adhesion defects that result in the relaxation of local mechanical conflicts, and pectin deficiency seems to have a direct effect on microtubule organization in plant cells (Verger et al., 2019). Therefore, it is unclear whether the defect of cellulose deposition in *QUA2* mutant seeds might also result from perturbed functional interplays between pectin and microtubules, which in turn influence cellulose synthesis. These questions will be the subject of future investigations into the connections between pectin and cellulose during seed development and germination, as well as in other developmental contexts.

In addition, our results reveal that seed germination in three mutants is inhibited under conditions of low water potential. This is potentially attributable to limited mucilage deposition and/or altered pectin methylesterification status

639 in the mutants, in connection with the fact that pectin is a highly hydratable
640 polymer and likely functions in mucilage to aid in water uptake during seed
641 germination (Muller et al., 2012). These data support the idea that the
642 production of mucilage is one strategy for plants to adapt to complex and
643 changing environments and efficiently acquire sufficient water for germination
644 (Western, 2012; Ezquer et al., 2016).

645 In summary, we found that the novel mutant allele *tfa2* and previously
646 characterized *tsd2* mutant display short hypocotyls and cell adhesion defects,
647 and significantly reduced seed mucilage extrusion after hydration. Biochemical
648 and immunolabeling analysis revealed the decreased uronic acid content and
649 lower degree of methylesterification in mucilage of *QUA2* mutants. We also
650 detected the decreased cellulose content and collapsed cellulosic rays in *tfa2*
651 and *tsd2* seeds. In the epidermal cells of *tfa2* and *tsd2* seed coat,
652 volcano-shaped columellae are deformed, displaying wider columella area and
653 thinner radial cell wall. Additionally, mutant seeds show reduced germination
654 rate after polyethylene glycol treatment. Together, these data demonstrate the
655 function of pectic HG biosynthesis mediated by QUA2 in the formation of seed
656 coat mucilage, and provide new evidence of how pectin HG together with
657 cellulose regulates seed mucilage formation and, consequently, seed
658 germination under detrimental conditions.

659 ## Acknowledgments

660 The authors thank Tanya Falbel and Sara Patterson for kindly providing
661 seeds of *tfa2*, *qua2*, and *tsd2* mutants. This work was supported by the
662 Institutional Research Fund from Sichuan University (2020SCUNL106), the
663 National Natural Science Foundation of China (32170357), and the
664 Fundamental Research Funds for the Central Universities (SCU2021D006) to
665 C.X.; Joint Science and Technology Support Program of Sichuan University
666 and Panzhihua City (2019CDPZH-19) to J.D. Writing contributions by C.T.A.

were supported by the Center for Lignocellulose Structure and Formation, an Energy Frontier Research Center funded by US DOE, Office of Science, Basic Energy Sciences under Award # DE-SC0001090.

## Author contributions

C.X. and J.D. designed the research; J.D., M.R., X.L., Q.L., Q.Z., S.H., and X.G. performed research; J.D., M.R., and C.X. analyzed data; J.D., M.R., C.T.A., and C.X. wrote the article.

## Declaration of competing interest

The authors declare that they have no conflicts of interest.

## References

Amos, R.A., Pattathil, S., Yang, J.Y., Atmodjo, M.A., Urbanowicz, B.R., Moremen, K.W., and Mohnen, D., 2018. A two-phase model for the non-processive biosynthesis of homogalacturonan polysaccharides by the GAUT1:GAUT7 complex. Journal of Biological Chemistry 293, 19047-19063.

Anderson, C.T., and Kieber, J.J., 2020. Dynamic construction, perception, and remodeling of plant cell walls. Annu Rev Plant Biol 71, 39-69.

Anderson, C.T., Carroll, A., Akhmetova, L., and Somerville, C., 2010. Real-time imaging of cellulose reorientation during cell wall expansion in Arabidopsis roots. Plant Physiol 152, 787-796.

Arsovski, A.A., Haughn, G.W., and Western, T.L., 2010. Seed coat mucilage cells of Arabidopsis thaliana as a model for plant cell wall research. Plant Signal Behav 5, 796-801.

Arsovski, A.A., Popma, T.M., Haughn, G.W., Carpita, N.C., McCann, M.C., and Western, T.L., 2009. AtBXL1 encodes a bifunctional beta-D-xylosidase/alpha-L-arabinofuranosidase required for pectic arabinan modification in Arabidopsis mucilage secretory cells. Plant Physiol 150, 1219-1234.

Atmodjo, M.A., Hao, Z.Y., and Mohnen, D., 2013. Evolving views of pectin biosynthesis. Annual Review of Plant Biology, Vol 64 64, 747-779.

Atmodjo, M.A., Sakuragi, Y., Zhu, X., Burrell, A.J., Mohanty, S.S., Atwood, J.A., 3rd, Orlando, R., Scheller, H.V., and Mohnen, D., 2011. Galacturonosyltransferase (GAUT)1 and GAUT7 are the core of a plant cell wall pectin biosynthetic homogalacturonan:galacturonosyltransferase complex. Proc Natl Acad Sci USA 108, 20225-20230.

Ben-Tov, D., Abraham, Y., Stav, S., Thompson, K., Loraine, A., Elbaum, R., de Souza, A., Pauly, M., Kieber, J.J., and Harpaz-Saad, S., 2015. COBRA-LIKE2, a member of the

glycosylphosphatidylinositol-anchored COBRA-LIKE family, plays a role in cellulose deposition in arabidopsis seed coat mucilage secretory cells. Plant Physiol 167, 711-724.

Bouton, S., Leboeuf, E., Mouille, G., Leydecker, M.T., Talbotec, J., Granier, F., Lahaye, M., Hofte, H., and Truong, H.N., 2002. QUASIMODO1 encodes a putative membrane-bound glycosyltransferase required for normal pectin synthesis and cell adhesion in Arabidopsis. Plant Cell 14, 2577-2590.

Caffall, K.H., and Mohnen, D., 2009. The structure, function, and biosynthesis of plant cell wall pectic polysaccharides. Carbohydr Res 344, 1879-1900.

Caffall, K.H., Pattathil, S., Phillips, S.E., Hahn, M.G., and Mohnen, D., 2009. Arabidopsis thaliana T-DNA mutants implicate GAUT genes in the biosynthesis of pectin and xylan in cell walls and seed testa. Mol Plant 2, 1000-1014.

Chiniquy, D., Underwood, W., Corwin, J., Ryan, A., Szemenyei, H., Lim, C.C., Stonebloom, S.H., Birdseye, D.S., Vogel, J., Kliebenstein, D., Scheller, H.V., and Somerville, S., 2019. PMR5, an acetylation protein at the intersection of pectin biosynthesis and defense against fungal pathogens. Plant J 100, 1022-1035.

Clough, S.J., and Bent, A.F., 1998. Floral dip: a simplified method for Agrobacterium-mediated transformation of Arabidopsis thaliana. Plant J 16, 735-743.

Dean, G.H., Zheng, H., Tewari, J., Huang, J., Young, D.S., Hwang, Y.T., Western, T.L., Carpita, N.C., McCann, M.C., Mansfield, S.D., and Haughn, G.W., 2007. The Arabidopsis MUM2 gene encodes a beta-galactosidase required for the production of seed coat mucilage with correct hydration properties. Plant Cell 19, 4007-4021.

Du, J., Kirui, A., Huang, S., Wang, L., Barnes, W.J., Kiemle, S.N., Zheng, Y., Rui, Y., Ruan, M., Qi, S., Kim, S.H., Wang, T., Cosgrove, D.J., Anderson, C.T., and Xiao, C., 2020. Mutations in the pectin methyltransferase QUASIMODO2 influence cellulose biosynthesis and wall integrity in Arabidopsis. Plant Cell 32, 3576-3597.

Ezquer, I., Mizzotti, C., Nguema-Ona, E., Gotte, M., Beauzamy, L., Viana, V.E., Dubrulle, N., Costa de Oliveira, A., Caporali, E., Koroney, A.S., Boudaoud, A., Driouich, A., and Colombo, L., 2016. The developmental regulator SEEDSTICK controls structural and mechanical properties of the Arabidopsis seed coat. Plant Cell 28, 2478-2492.

Francoz, E., Ranocha, P., Burlat, V., and Dunand, C., 2015. Arabidopsis seed mucilage secretory cells: regulation and dynamics. Trends Plant Sci 20, 515-524.

Goubet, F., and Mohnen, D., 1999. Solubilization and partial characterization of homogalacturonan-methyltransferase from microsomal membranes of suspension-cultured tobacco cells. Plant Physiol 121, 281-290.

Griffiths, J.S., and North, H.M., 2017. Sticking to cellulose: exploiting Arabidopsis seed coat mucilage to understand cellulose biosynthesis and cell wall polysaccharide interactions. New Phytol 214, 959-966.

Griffiths, J.S., Tsai, A.Y., Xue, H., Voiniciuc, C., Sola, K., Seifert, G.J., Mansfield, S.D., and Haughn, G.W., 2014. SALT-OVERLY SENSITIVE5 mediates Arabidopsis seed coat mucilage adherence and organization through pectins. Plant Physiol 165, 991-1004.

Griffiths, J.S., Sola, K., Kushwaha, R., Lam, P., Tateno, M., Young, R., Voiniciuc, C., Dean, G., Mansfield, S.D., DeBolt, S., and Haughn, G.W., 2015. Unidirectional movement of cellulose synthase complexes in Arabidopsis seed coat epidermal cells deposit cellulose involved in mucilage extrusion, adherence, and ray formation. Plant Physiol 168, 502-520.

746 Hao, Z., Avci, U., Tan, L., Zhu, X., Glushka, J., Pattathil, S., Eberhard, S., Sholes, T., Rothstein,
747 G.E., Lukowitz, W., Orlando, R., Hahn, M.G., and Mohnen, D., 2014. Loss of Arabidopsis
748 GAUT12/IRX8 causes anther indehiscence and leads to reduced G lignin associated with
749 altered matrix polysaccharide deposition. Front Plant Sci 5, 357.
750 Harpaz-Saad, S., Western, T.L., and Kieber, J.J., 2012. The FEI2-SOS5 pathway and
751 CELLULOSE SYNTHASE 5 are required for cellulose biosynthesis in the Arabidopsis
752 seed coat and affect pectin mucilage structure. Plant Signal Behav 7, 285-288.
753 Haughn, G.W., and Western, T.L., 2012. Arabidopsis seed coat mucilage is a specialized cell
754 wall that can be used as a model for genetic analysis of plant cell wall structure and
755 function. Front Plant Sci 3, 64.
756 Hocq, L., Pelloux, J., and Lefebvre, V., 2017. Connecting homogalacturonan-type pectin
757 remodeling to acid growth. Trends Plant Sci 22, 20-29.
758 Hu, R., Li, J., Wang, X., Zhao, X., Yang, X., Tang, Q., He, G., Zhou, G., and Kong, Y., 2016.
759 Xylan synthesized by irregular xylem 14 (IRX14) maintains the structure of seed coat
760 mucilage in Arabidopsis. J Exp Bot 67, 1243-1257.
761 Kim, S.J., Held, M.A., Zemelis, S., Wilkerson, C., and Brandizzi, F., 2015. CGR2 and CGR3
762 have critical overlapping roles in pectin methylesterification and plant growth in
763 Arabidopsis thaliana. Plant J 82, 208-220.
764 Klavons, J.A., and Bennett, R.D., 1986. Determination of methanol using alcohol oxidase and
765 its application to methyl-ester content of pectins. J Agr Food Chem 34, 597-599.
766 Krupkova, E., Immerzeel, P., Pauly, M., and Schmulling, T., 2007. The TUMOROUS SHOOT
767 DEVELOPMENT2 gene of Arabidopsis encoding a putative methyltransferase is required
768 for cell adhesion and co-ordinated plant development. Plant J 50, 735-750.
769 Le, B.H., Cheng, C., Bui, A.Q., Wagmaister, J.A., Henry, K.F., Pelletier, J., Kwong, L.,
770 Belmonte, M., Kirkbride, R., Horvath, S., Drews, G.N., Fischer, R.L., Okamuro, J.K.,
771 Harada, J.J., and Goldberg, R.B., 2010. Global analysis of gene activity during
772 Arabidopsis seed development and identification of seed-specific transcription factors.
773 Proc Natl Acad Sci U S A 107, 8063-8070.
774 Louvet, R., Rayon, C., Domon, J.M., Rusterucci, C., Fournet, F., Leaustic, A., Crepeau, M.J.,
775 Ralet, M.C., Rihouey, C., Bardor, M., Lerouge, P., Gillet, F., and Pelloux, J., 2011. Major
776 changes in the cell wall during silique development in Arabidopsis thaliana.
777 Phytochemistry 72, 59-67.
778 Macquet, A., Ralet, M.C., Kronenberger, J., Marion-Poll, A., and North, H.M., 2007. In situ,
779 chemical and macromolecular study of the composition of Arabidopsis thaliana seed coat
780 mucilage. Plant Cell Physiol 48, 984-999.
781 Mendu, V., Griffiths, J.S., Persson, S., Stork, J., Downie, A.B., Voiniciuc, C., Haughn, G.W.,
782 and DeBolt, S., 2011. Subfunctionalization of cellulose synthases in seed coat epidermal
783 cells mediates secondary radial wall synthesis and mucilage attachment. Plant Physiol
784 157, 441-453.
785 Miao, Y., Li, H.Y., Shen, J., Wang, J., and Jiang, L., 2011. QUASIMODO 3 (QUA3) is a putative
786 homogalacturonan methyltransferase regulating cell wall biosynthesis in Arabidopsis
787 suspension-cultured cells. J Exp Bot 62, 5063-5078.
788 Mizzotti, C., Ezquer, I., Paolo, D., Rueda-Romero, P., Guerra, R.F., Battaglia, R., Rogachev, I.,
789 Aharoni, A., Kater, M.M., Caporali, E., and Colombo, L., 2014. SEEDSTICK is a master

790 regulator of development and metabolism in the Arabidopsis seed coat. PLoS Genet 10,
791 e1004856.
792 Mohnen, D., 2008. Pectin structure and biosynthesis. Curr Opin Plant Biol 11, 266-277.
793 Mouille, G., Ralet, M.C., Cavelier, C., Eland, C., Effroy, D., Hematy, K., McCartney, L., Truong,
794 H.N., Gaudon, V., Thibault, J.F., Marchant, A., and Hofte, H., 2007. Homogalacturonan
795 synthesis in Arabidopsis thaliana requires a Golgi-localized protein with a putative
796 methyltransferase domain. Plant J 50, 605-614.
797 Muller, K., Levesque-Tremblay, G., Bartels, S., Weitbrecht, K., Wormit, A., Usadel, B., Haughn,
798 G., and Kermode, A.R., 2012. Demethylesterification of cell wall pectins in Arabidopsis
799 plays a role in seed germination. Plant Physiol 161, 305-316.
800 Oka, T., Nemoto, T., and Jigami, Y., 2007. Functional analysis of Arabidopsis thaliana
801 RHM2/MUM4, a multidomain protein involved in UDP-D-glucose to UDP-L-rhamnose
802 conversion. J Biol Chem 282, 5389-5403.
803 Peaucelle, A., Braybrook, S., and Hofte, H., 2012. Cell wall mechanics and growth control in
804 plants: the role of pectins revisited. Front Plant Sci 3, 121.
805 Pelloux, J., Rusterucci, C., and Mellerowicz, E.J., 2007. New insights into pectin
806 methylesterase structure and function. Trends Plant Sci 12, 267-277.
807 Persson, S., Caffall, K.H., Freshour, G., Hilley, M.T., Bauer, S., Poindexter, P., Hahn, M.G.,
808 Mohnen, D., and Somerville, C., 2007. The Arabidopsis irregular xylem8 mutant is
809 deficient in glucuronoxylan and homogalacturonan, which are essential for secondary cell
810 wall integrity. Plant Cell 19, 237-255.
811 Qu, L., Wu, C., Zhang, F., Wu, Y., Fang, C., Jin, C., Liu, X., and Luo, J., 2016. Rice putative
812 methyltransferase gene OsTSD2 is required for root development involving pectin
813 modification. J Exp Bot 67, 5349-5362.
814 Rautengarten, C., Usadel, B., Neumetzler, L., Hartmann, J., Bussis, D., and Altmann, T., 2008.
815 A subtilisin-like serine protease essential for mucilage release from Arabidopsis seed
816 coats. Plant J 54, 466-480.
817 Rui, Y., Xiao, C., Hojae, Kandemir, B., Wang, J.Z., Puri, V.M., and Anderson, C.T., 2017.
818 POLYGALACTURONASE INVOLVED IN EXPANSION3 functions in seedling
819 development, rosette growth, and stomatal dynamics in Arabidopsis thaliana. Plant Cell
820 29, 2413-2432.
821 Saez-Aguayo, S., Ralet, M.C., Berger, A., Botran, L., Ropartz, D., Marion-Poll, A., and North,
822 H.M., 2013. PECTIN METHYLESTERASE INHIBITOR6 promotes Arabidopsis mucilage
823 release by limiting methylesterification of homogalacturonan in seed coat epidermal cells.
824 Plant Cell 25, 308-323.
825 Sola, K., Gilchrist, E.J., Ropartz, D., Wang, L., Feussner, I., Mansfield, S.D., Ralet, M.C., and
826 Haughn, G.W., 2019. RUBY, a putative galactose oxidase, influences pectin properties
827 and promotes cell-to-cell adhesion in the seed coat epidermis of Arabidopsis. Plant Cell
828 31, 809-831.
829 Staehelin, L.A., and Moore, I., 1995. The plant Golgi-apparatus - structure,
830 functional-organization and trafficking mechanisms. Annual Review of Plant Physiology
831 and Plant Molecular Biology 46, 261-288.
832 Stork, J., Harris, D., Griffiths, J., Williams, B., Beisson, F., Li-Beisson, Y., Mendu, V., Haughn,
833 G., and DeBolt, S., 2010. CELLULOSE SYNTHASE9 serves a nonredundant role in

834 secondary cell wall synthesis in Arabidopsis epidermal testa cells. Plant Physiol 153,
835 580-589.
836 Sullivan, S., Ralet, M.C., Berger, A., Diatloff, E., Bischoff, V., Gonneau, M., Marion-Poll, A., and
837 North, H.M., 2011. CESA5 is required for the synthesis of cellulose with a role in
838 structuring the adherent mucilage of Arabidopsis seeds. Plant Physiol 156, 1725-1739.
839 Updegraff, D.M., 1969. Semimicro determination of cellulose in biological materials. Anal
840 Biochem 32, 420-424.
841 Usadel, B., Kuschinsky, A.M., Rosso, M.G., Eckermann, N., and Pauly, M., 2004. RHM2 is
842 involved in mucilage pectin synthesis and is required for the development of the seed coat
843 in Arabidopsis. Plant Physiol 134, 286-295.
844 Vaahtera, L., Schulz, J., and Hamann, T., 2019. Cell wall integrity maintenance during plant
845 development and interaction with the environment. Nat Plants 5, 924-932.
846 Verger, S., Liu, M., and Hamant, O., 2019. Mechanical conflicts in twisting growth revealed by
847 cell-cell adhesion defects. Front Plant Sci 10, 173.
848 Voiniciuc, C., Gunl, M., Schmidt, M.H., and Usadel, B., 2015a. Highly branched xylan made by
849 IRREGULAR XYLEM14 and MUCILAGE-RELATED21 links mucilage to Arabidopsis
850 seeds. Plant Physiol 169, 2481-2495.
851 Voiniciuc, C., Schmidt, M.H.W., Berger, A., Yang, B., Ebert, B., Scheller, H.V., North, H.M.,
852 Usadel, B., and Gunl, M., 2015b. MUCILAGE-RELATED10 produces
853 galactoglucomannan that maintains pectin and cellulose architecture in Arabidopsis seed
854 mucilage. Plant Physiol 169, 403-420.
855 Voiniciuc, C., Engle, K.A., Gunl, M., Dieluweit, S., Schmidt, M.H., Yang, J.Y., Moremen, K.W.,
856 Mohnen, D., and Usadel, B., 2018. Identification of key enzymes for pectin synthesis in
857 seed mucilage. Plant Physiol 178, 1045-1064.
858 Voiniciuc, C., Dean, G.H., Griffiths, J.S., Kirchsteiger, K., Hwang, Y.T., Gillett, A., Dow, G.,
859 Western, T.L., Estelle, M., and Haughn, G.W., 2013. FLYING SAUCER1 is a
860 transmembrane RING E3 ubiquitin ligase that regulates the degree of pectin
861 methylesterification in Arabidopsis seed mucilage. Plant Cell 25, 944-959.
862 Western, T.L., 2012. The sticky tale of seed coat mucilages: production, genetics, and role in
863 seed germination and dispersal. Seed Science Research 22, 1-25.
864 Western, T.L., Skinner, D.J., and Haughn, G.W., 2000. Differentiation of mucilage secretory
865 cells of the Arabidopsis seed coat. Plant Physiol 122, 345-356.
866 Western, T.L., Young, D.S., Dean, G.H., Tan, W.L., Samuels, A.L., and Haughn, G.W., 2004.
867 MUCILAGE-MODIFIED4 encodes a putative pectin biosynthetic enzyme developmentally
868 regulated by APETALA2, TRANSPARENT TESTA GLABRA1, and GLABRA2 in the
869 Arabidopsis seed coat. Plant Physiol 134, 296-306.
870 Willats, W.G., Orfila, C., Limberg, G., Buchholt, H.C., van Alebeek, G.J., Voragen, A.G.,
871 Marcus, S.E., Christensen, T.M., Mikkelsen, J.D., Murray, B.S., and Knox, J.P., 2001.
872 Modulation of the degree and pattern of methyl-esterification of pectic homogalacturonan
873 in plant cell walls. Implications for pectin methyl esterase action, matrix properties, and
874 cell adhesion. J Biol Chem 276, 19404-19413.
875 Windsor, J.B., Symonds, V.V., Mendenhall, J., and Lloyd, A.M., 2000. Arabidopsis seed coat
876 development: morphological differentiation of the outer integument. Plant J 22, 483-493.
877 Winter, D., Vinegar, B., Nahal, H., Ammar, R., Wilson, G.V., and Provart, N.J., 2007. An

"Electronic Fluorescent Pictograph" browser for exploring and analyzing large-scale biological data sets. Plos One 2, e718.

Wolf, S., Mouille, G., and Pelloux, J., 2009. Homogalacturonan methyl-esterification and plant development. Mol Plant 2, 851-860.

Wu, Q., Li, Y., Lyu, M., Luo, Y., Shi, H., and Zhong, S., 2020. Touch-induced seedling morphological changes are determined by ethylene-regulated pectin degradation. Sci Adv 6, eabc9294.

Xiao, C., Somerville, C., and Anderson, C.T., 2014. POLYGALACTURONASE INVOLVED IN EXPANSION1 functions in cell elongation and flower development in Arabidopsis. Plant Cell 26, 1018-1035.

Xiao, C.W., Zhang, T., Zheng, Y.Z., Cosgrove, D.J., and Anderson, C.T., 2016. Xyloglucan deficiency disrupts microtubule stability and cellulose biosynthesis in Arabidopsis, altering cell growth and morphogenesis. Plant Physiol 170, 234-249.

Xu, Y., Wang, Y., Wang, X., Pei, S., Kong, Y., Hu, R., and Zhou, G., 2020. Transcription factors BLH2 and BLH4 regulate demethylesterification of homogalacturonan in seed mucilage. Plant Physiol 183, 96-111.

Xu, Y., Wang, Y., Du, J., Pei, S., Guo, S., Hao, R., Wang, D., Zhou, G., Li, S., O'Neill, M., Hu, R., and Kong, Y., 2022. A DE1 BINDING FACTOR 1-GLABRA2 module regulates rhamnogalacturonan I biosynthesis in Arabidopsis seed coat mucilage. Plant Cell koac011.

Yang, B., Voiniciuc, C., Fu, L.B., Dieluweit, S., Klose, H., and Usadel, B., 2019. TRM4 is essential for cellulose deposition in Arabidopsis seed mucilage by maintaining cortical microtubule organization and interacting with CESA3. New Phytologist 221, 881-895.

Zablackis, E., Huang, J., Muller, B., Darvill, A.G., and Albersheim, P., 1995. Characterization of the cell-wall polysaccharides of Arabidopsis thaliana leaves. Plant Physiol 107, 1129-1138.

# Figure Legends

**Fig. 1.** *tfa2* seedlings have shorter hypocotyls and cell adhesion defects together with *tsd2* and *qua2* mutants. **(A)** Schematic gene structure of *QUASIMODO2* (exons shown as solid boxes, introns as gray lines, 5′ and 3′ regions as gray boxes) with three different point mutations. *tsd2* and *qua2* are presented by Krupkova et al., 2007 and Mouille et al., 2007, respectively. *tfa2* contains a point mutation in the third exon of *QUA2* gene, which results in premature termination. **(B)** Six-day-old etiolated seedlings of Col, *tfa2*, *tsd2*, and *qua2* grown in the dark. Scale bar, 1 cm. **(C)** Hypocotyl length of Col, *tfa2*, *tsd2*, and *qua2* seedlings grown in dark for 6 days ($n \geq 20$ seedlings per genotype), at least three replicates were performed. Bars represent SD, and asterisks indicate significant differences (**$P < 0.001$, *t*-test). **(D)** *tfa2*, *tsd2*, and *qua2* mutant alleles display different levels of cell adhesion defects. Scale bar, 200 μm.

**Fig. 2.** *tfa2* and *tsd2* mutants have altered water absorption capability. **(A, B)** One hundred milligrams dry seeds of Col, *tfa2*, *tsd2*, and *qua2* mutants before **(A)** and after **(B)** soaking in 1 mL water overnight at room temperature. Scale bar, 1 cm. **(C)** Heights of

seeds in each tube after soaking in water ($n$ = 3 tubes per genotype). **(D)** Sizes of dry seeds from Col, *tfa2*, *tsd2*, and *qua2* mutants ($n \geq 80$ seeds per genotype). Bars represent SD, and asterisk indicates significant difference (**$P < 0.001$, *t*-test).

**Fig. 3.** *QUA2* mutants display aberrant seed coat mucilage. **(A)** Seeds of Col, *tfa2*, *tsd2*, and *qua2* mutants were hydrated in water and stained with ruthenium red (RR) for 45 min and visualized by stereomicroscope. Scale bar, 100 μm. **(B)** Quantification of RR-stained mucilage area in seeds ($n \geq 100$ seeds per genotype). **(C)** Measurement of adherent mucilage weight from seeds of Col, *tfa2*, *tsd2*, and *qua2* mutants ($n$ = 3 technical replicates per genotype). Bars represent SD, and asterisks indicate significant differences (**$P < 0.001$, *t*-test).

**Fig. 4.** Biochemical determination and immunolabeling of pectin methylesterification in whole seeds and mucilage from wild-type and mutants. **(A)** Total uronic acid content in extracted mucilage from Col and mutant seeds. **(B)** Methanol content in extracted mucilage from Col and mutants seeds. **(C)** Degree of pectin methylesterification of extracted mucilage from Col and mutant seeds calculated as the ratio of methanol to uronic acid ($n$ = 5 technical replicates per genotype). **(D)** Immunolabeling of intact seeds with JIM5 and JIM7, which are antibodies that recognize low-methylesterified and high-methylesterifed HG, respectively. Scale bar, 100 μm. **(E, F)** Arbitrary fluorescent intensity of immunolabeling images for JIM5 and JIM7 antibodies ($n \geq 8$). Bars represent SD, and asterisks indicate significant differences (*$P < 0.05$, **$P < 0.001$, *t*-test).

**Fig. 5.** Cellulose deposition is defective in *QUA2* mutant alleles. **(A)** Crystalline cellulose content was decreased in mutant seeds compared with Col controls ($n$ = 5 technical replicates per genotype). **(B)** S4B and Calcoflour White staining of cellulose in mucilage capsules of seeds hydrated in water. Scale bar, 100 μm. **(C, D)** Arbitrary fluorescence intensities of cellulosic rays from S4B staining **(C)** and Calcoflour White **(D)** staining images, respectively ($n$ = 10 seeds per genotype). Bars represent SD, and asterisks indicate significant differences (*$P < 0.05$, **$P < 0.001$, *t*-test).

**Fig. 6.** Columella imaging of dry mature seeds of wild-type and mutants. **(A, B)** The surface morphology of dry *tfa2* and *tsd2* seeds show more flat volcano-shaped columellae that differ from Col controls. **(C)** Zoomed images from **(B)** show the center of single volcano-shaped columella in wild-type and mutant seeds. **(D, E)** Quantification of columella area and radial cell wall thickness from the images in **(C)** ($n \geq 124$ cells per genotype). **(F)** Images of mature seeds showing volcano-shaped columella cells in confocal microscope. **(G)** Zoomed images from **(F)**. Scale bar, 100 μm in **(A, F, G)**, 50 μm in **(B)**, and 25 μm in **(C)**. Bars represent SD, and asterisks indicate significant differences (**$P < 0.001$, *t*-test).

**Fig. 7.** Seed germination rate of *QUA2* mutants is decreased with the treatment of polyethylene glycol (PEG). Water (control) or 10% PEG (PEG) was used to treat Col and mutant seeds ($n \geq 100$ seeds from three biological replicates). Seed germination rate was scored every 12 h. HAS, hours after sowing. Asterisks indicate significant differences (*$P < 0.05$, *t*-test).

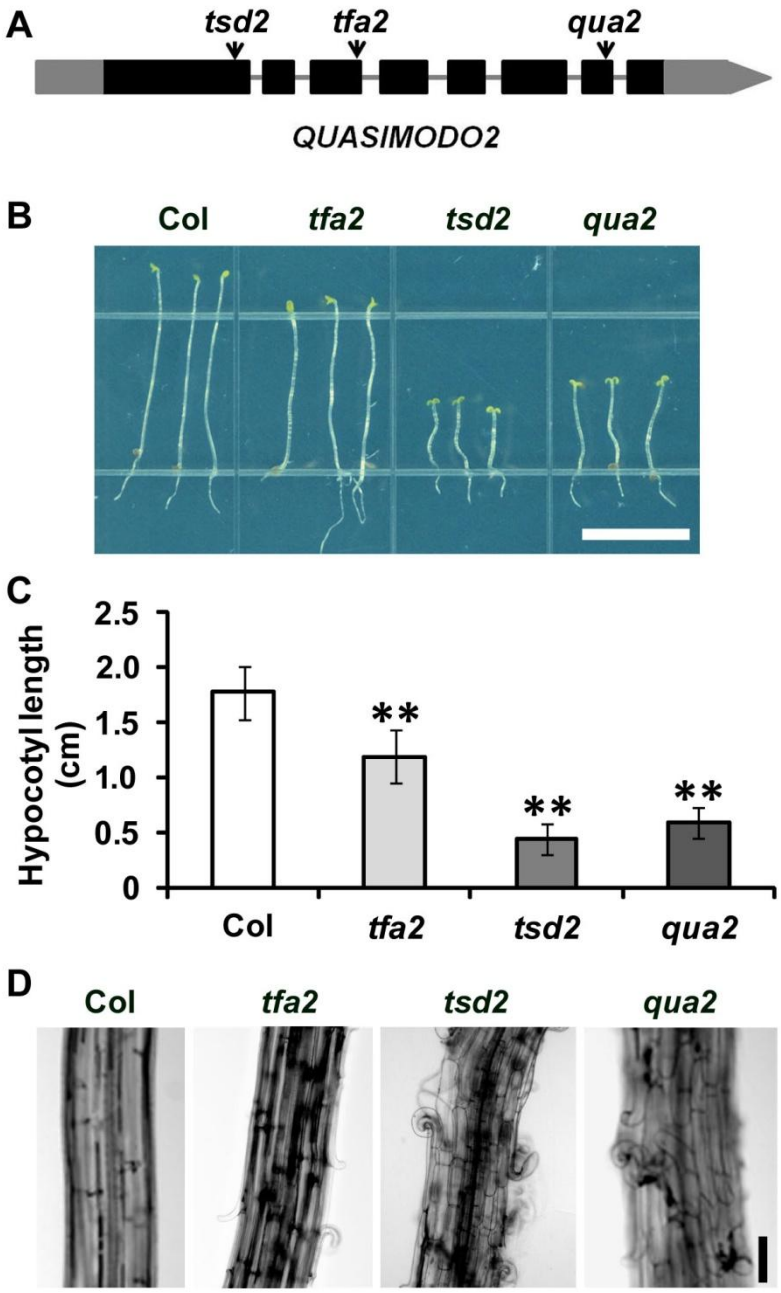


**Fig. 1.** *tfa2* seedlings have shorter hypocotyls and cell adhesion defects together with *tsd2* and *qua2* mutants. **(A)** Schematic gene structure of *QUASIMODO2* (exons shown as solid boxes, introns as gray lines, 5′ and 3′ regions as gray boxes) with three different point mutations. *tsd2* and *qua2* are presented by Krupkova et al., 2007 and Mouille et al., 2007, respectively. *tfa2* contains a point mutation in the third exon of *QUA2* gene, which results in premature termination. **(B)** Six-day-old etiolated seedlings of Col, *tfa2*, *tsd2*, and *qua2* grown in the dark. Scale bar, 1 cm. **(C)** Hypocotyl length of Col, *tfa2*, *tsd2*, and *qua2* seedlings grown in dark for 6 days ($n \geq 20$ seedlings per genotype), at least three replicates were performed. Bars represent SD, and asterisks indicate significant differences (**$P < 0.001$, *t*-test). **(D)** *tfa2*, *tsd2*, and *qua2* mutant alleles display different levels of cell adhesion defects. Scale bar, 200 μm.

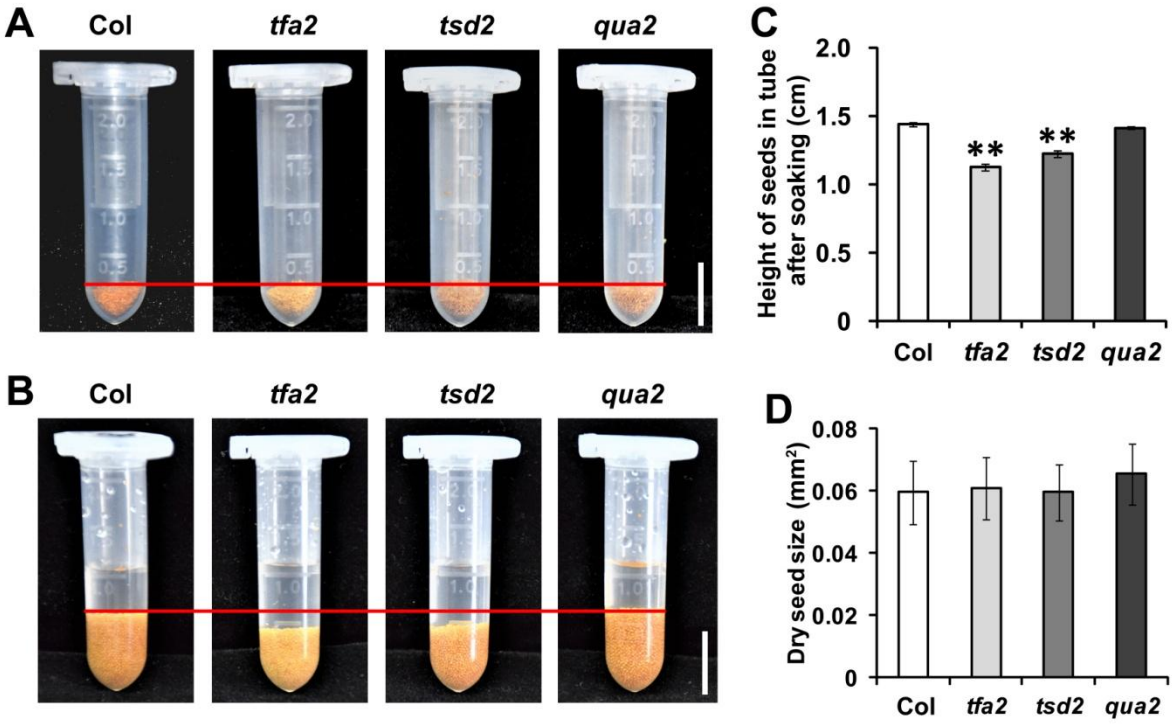


**Fig. 2.** *tfa2* and *tsd2* mutants have altered water absorption capability. **(A, B)** One hundred milligrams dry seeds of Col, *tfa2*, *tsd2*, and *qua2* mutants before **(A)** and after **(B)** soaking in 1 mL water overnight at room temperature. Scale bar, 1 cm. **(C)** Heights of seeds in each tube after soaking in water ($n$ = 3 tubes per genotype). **(D)** Sizes of dry seeds from Col, *tfa2*, *tsd2*, and *qua2* mutants ($n \geq 80$ seeds per genotype). Bars represent SD, and asterisk indicates significant difference (**$P < 0.001$, $t$-test).

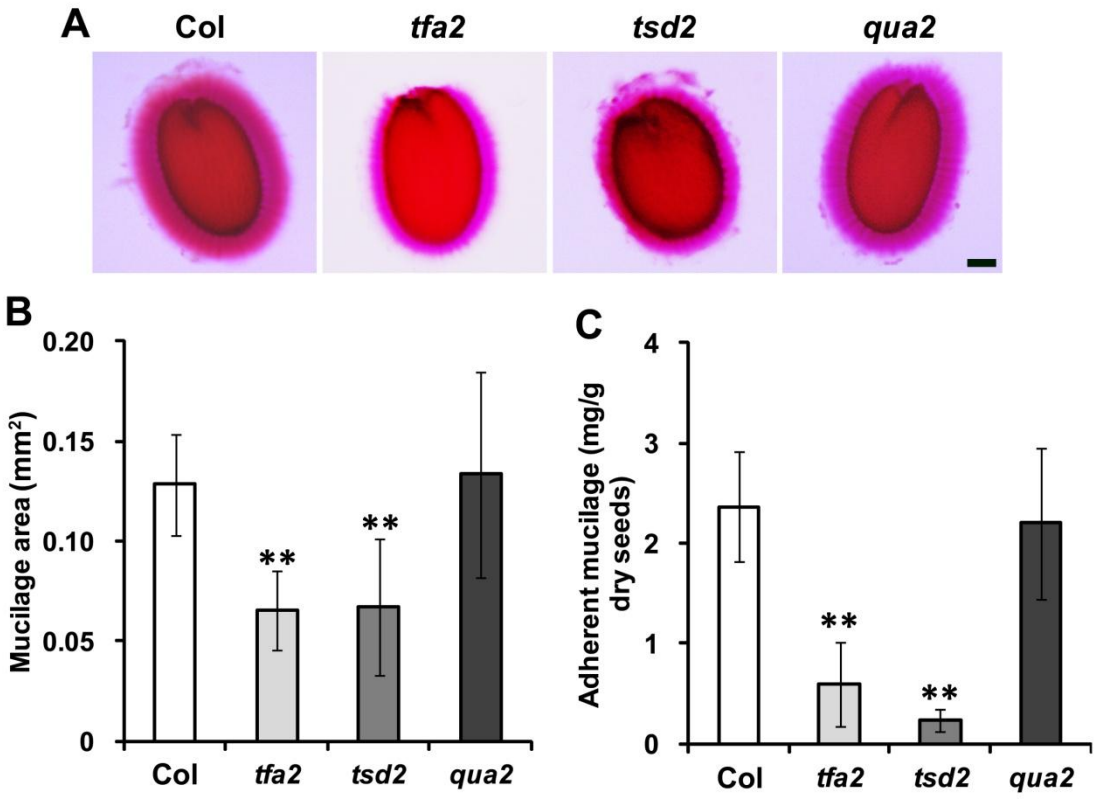


**Fig. 3.** *QUA2* mutants display aberrant seed coat mucilage. **(A)** Seeds of Col, *tfa2*, *tsd2*, and *qua2* mutants were hydrated in water and stained with ruthenium red (RR) for 45 min and visualized by stereomicroscope. Scale bar, 100 µm. **(B)** Quantification of RR-stained mucilage area in seeds ($n \geq 100$ seeds per genotype). **(C)** Measurement of adherent mucilage weight from seeds of Col, *tfa2*, *tsd2*, and *qua2* mutants ($n = 3$ technical replicates per genotype). Bars represent SD, and asterisks indicate significant differences (**$P < 0.001$, *t*-test).

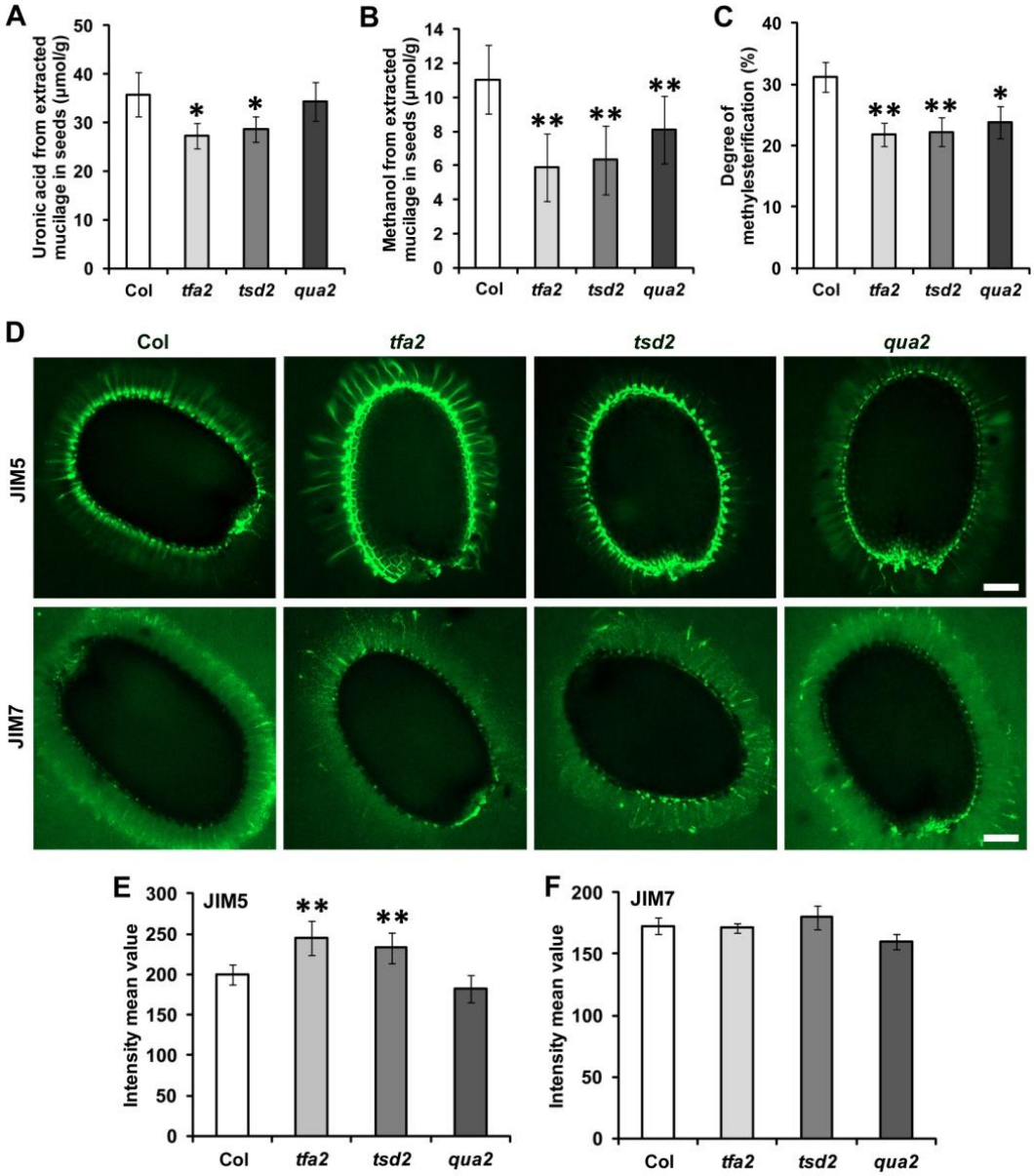


**Fig. 4.** Biochemical determination and immunolabeling of pectin methylesterification in whole seeds and mucilage from wild-type and mutants. **(A)** Total uronic acid content in extracted mucilage from Col and mutant seeds. **(B)** Methanol content in extracted mucilage from Col and mutants seeds. **(C)** Degree of pectin methylesterification of extracted mucilage from Col and mutant seeds calculated as the ratio of methanol to uronic acid ($n$ = 5 technical replicates per genotype). **(D)** Immunolabeling of intact seeds with JIM5 and JIM7, which are antibodies that recognize low-methylesterified and high-methylesterifed HG, respectively. Scale bar, 100 µm. **(E, F)** Arbitrary fluorescent intensity of immunolabeling images for JIM5 and JIM7 antibodies ($n \geq 8$). Bars represent SD, and asterisks indicate significant differences (*$P < 0.05$, **$P < 0.001$, $t$-test).

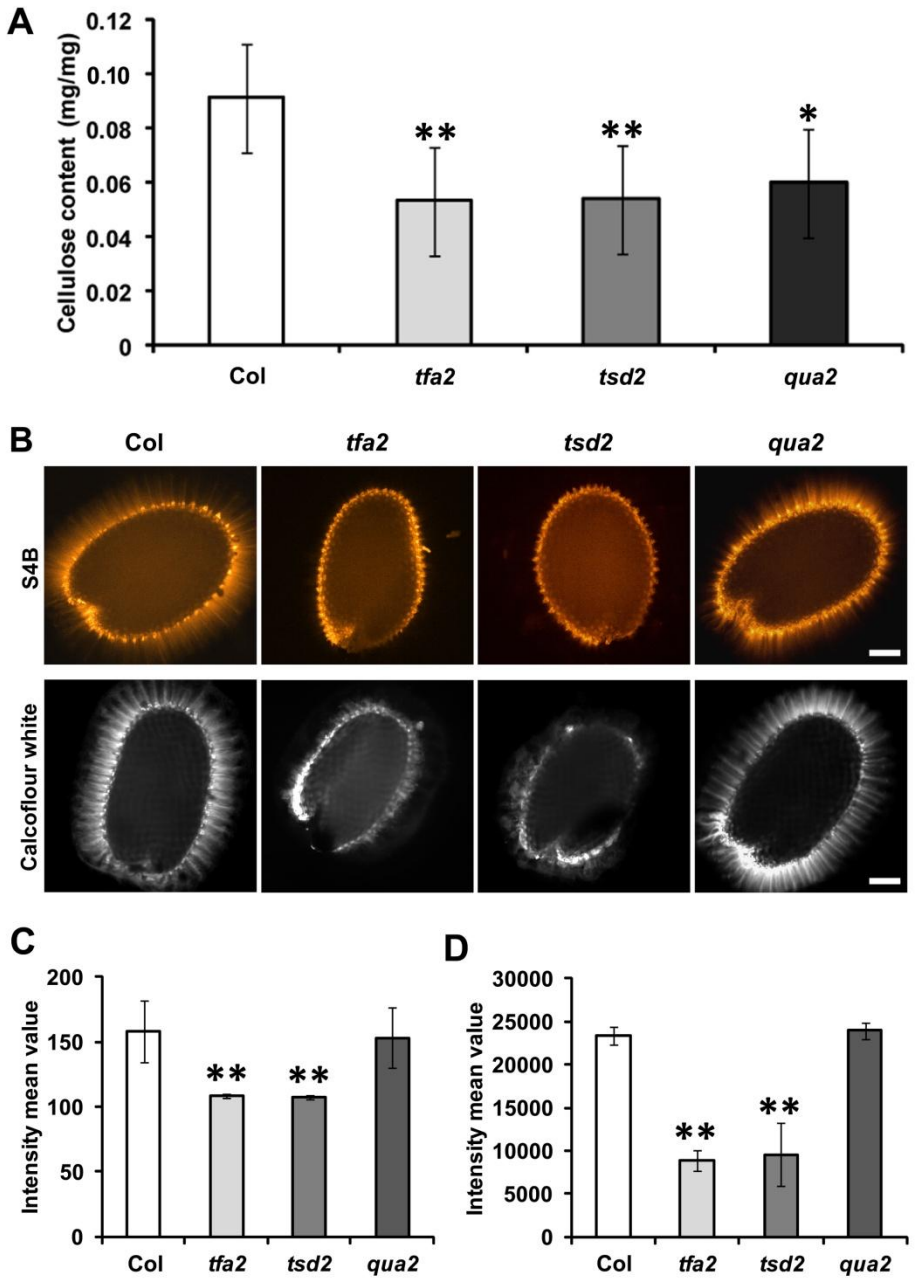


**Fig. 5.** Cellulose deposition is defective in *QUA2* mutant alleles. **(A)** Crystalline cellulose content was decreased in mutant seeds compared with Col controls ($n$ = 5 technical replicates per genotype). **(B)** S4B and Calcoflour White staining of cellulose in mucilage capsules of seeds hydrated in water. Scale bar, 100 µm. **(C, D)** Arbitrary fluorescence intensities of cellulosic rays from S4B staining **(C)** and Calcoflour White **(D)** staining images, respectively ($n$ = 10 seeds per genotype). Bars represent SD, and asterisks indicate significant differences (*$P$ < 0.05, **$P$ < 0.001, $t$-test).

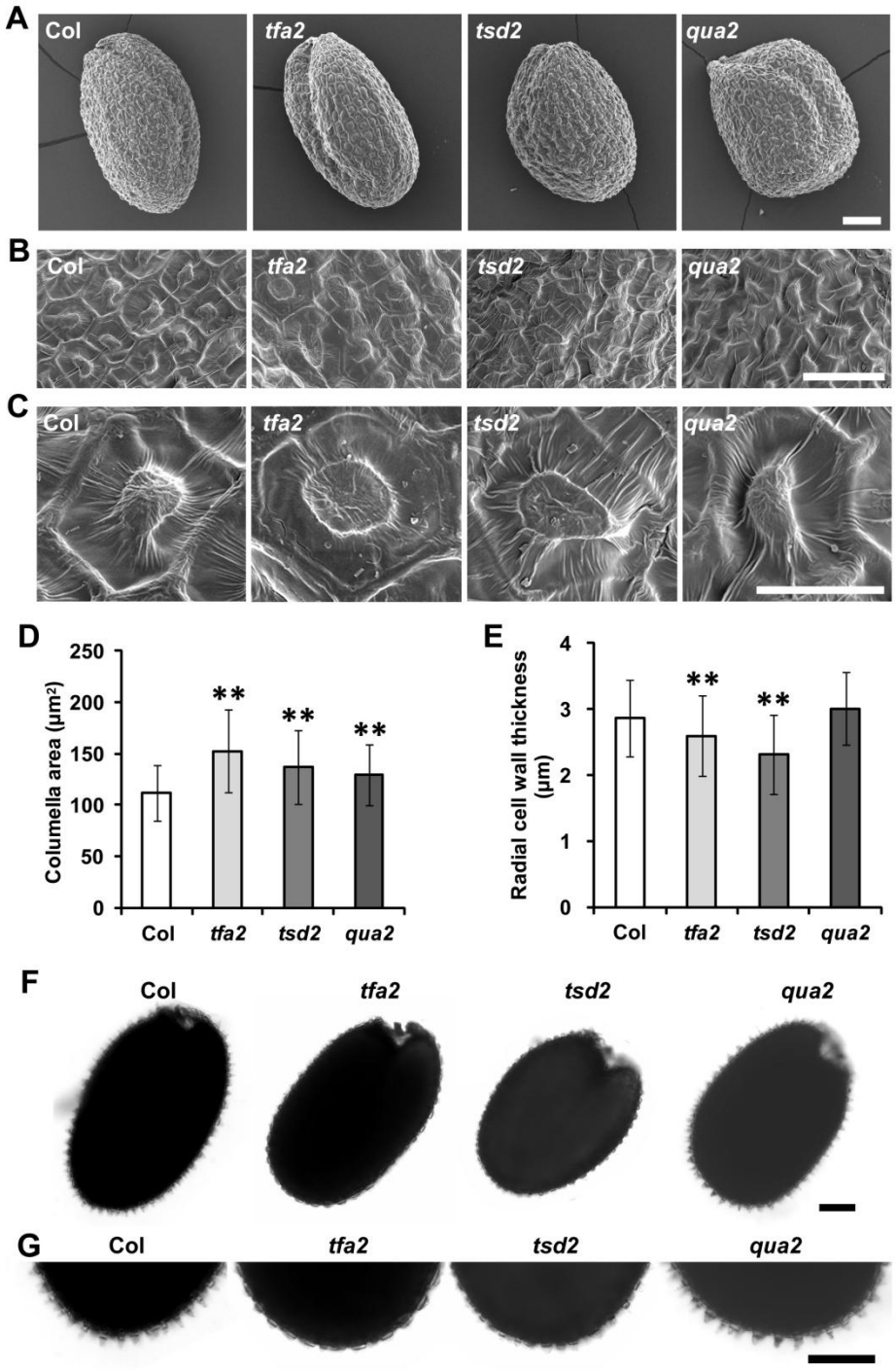


**Fig. 6.** Columella imaging of dry mature seeds of wild-type and mutants. **(A, B)** The surface morphology of dry *tfa2* and *tsd2* seeds show more flat volcano-shaped columellae that differ from Col controls. **(C)** Zoomed images from **(B)** show the center of single volcano-shaped columella in wild-type and mutant seeds. **(D, E)** Quantification of columella area and radial cell wall thickness from the images in **(C)** ($n \geq 124$ cells per genotype). **(F)** Images of mature seeds showing volcano-shaped columella cells in confocal microscope. **(G)** Zoomed images from **(F)**. Scale bar, 100 μm in **(A, F, G)**, 50 μm in **(B)**, and 25 μm in **(C)**. Bars represent SD, and asterisks indicate significant differences (**$P < 0.001$, *t*-test).

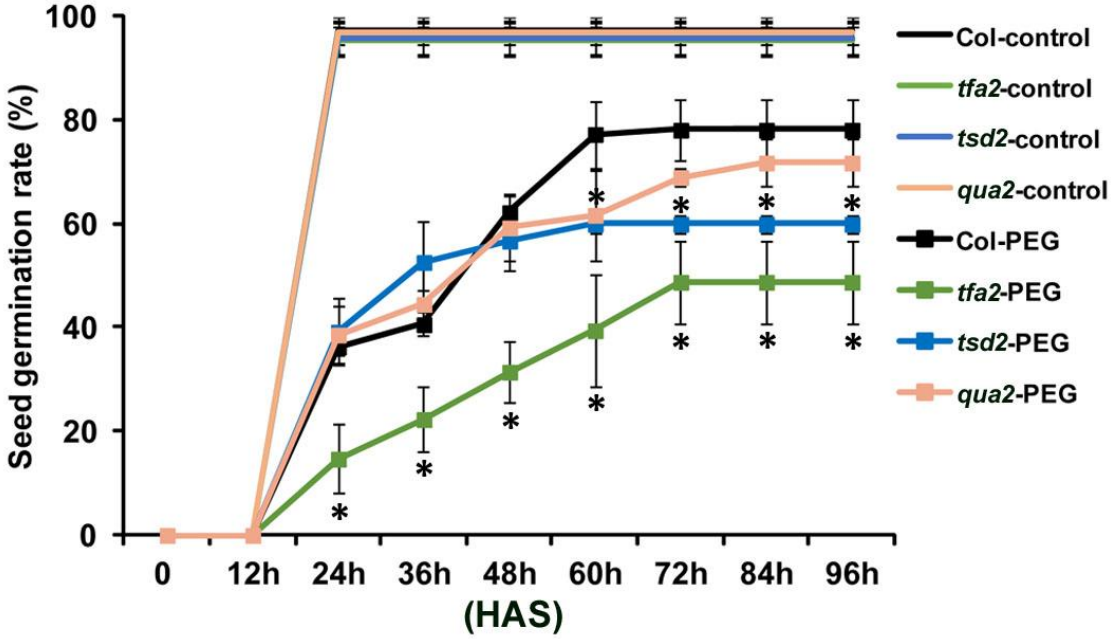


**Fig. 7.** Seed germination rate of *QUA2* mutants is decreased with the treatment of polyethylene glycol (PEG). Water (control) or 10% PEG (PEG) was used to treat Col and mutant seeds ($n \geq 100$ seeds from three biological replicates). Seed germination rate was scored every 12 h. HAS, hours after sowing. Asterisks indicate significant differences (*$P < 0.05$, *t*-test).